*Acta Cryst.* (1976). A32, 653

# Data Collection in Protein Crystallography: Experimental Methods for Reducing Background Radiation*

BY MONTY KRIEGER† AND ROBERT M. STROUD‡

*Norman W. Church Laboratory of Chemical Biology, California Institute of Technology, Pasadena, California* 91125, *U.S.A.*

(*Received* 13 *December* 1975; *accepted* 30 *January* 1976)

The primary source of background intensity when diffraction intensities are measured by diffractometry is air scatter from the volume of air irradiated by the direct X-ray beam which scatters incident radiation into the photon-detection system. In protein crystallography where crystals are generally enclosed in glass capillaries, scattering of the direct beam from the glass is the second most significant source of background intensity. Glass scattering leads to a broad diffuse ring centered at spacings of 3·0 Å ($2\theta$= 20–32°), whereas air scattering continuously diminishes in intensity between $2\theta=0°$ and 45° [Krieger, Chambers, Christoph, Stroud & Trus, (1974), *Acta Cryst.* A **30**, 740–748]. Compared to these sources of background radiation, other sources are usually insignificant. Two experimental methods are described which reduce the air-scattered component of backgrounds by as much as a factor of 100. Use of these methods increased the peak-to-background ratio by a factor of three–ten times in the case of typical diffractometry of protein crystals. This can be translated into time saving during data collection, and into an increase in the range of measurable intensities.

## Introduction

In X-ray crystallography, the speed and accuracy of data collection is ultimately limited by the signal-to-noise ratio. Rapid data collection is especially imtant in protein crystallography because the useful crystal exposure time is limited by crystal decay. If the signal-to-noise ratio can be maximized, more and better data can be collected from a single protein crystal.

Our first investigation (Krieger *et al.*, 1974) of background intensity in protein crystallography served to identify the primary sources: first, background radiation is produced by scatter from the volume (the 'visible volume') of air irradiated by the direct incident beam, and seen by the photon detector. This effect generally overwhelms all other sources in the range of $2\theta$ between 0° and 15° (*i.e.* within the ∞–6 Å resolution range). A second source is scatter from the glass capillary in which protein crystals are usually mounted. Capillary scatter becomes most significant in the range of $2\theta$ between 20° and 32°, and generally overwhelms any contribution from solvent around the protein crystal in the capillary, or from inelastically scattered photons from the protein crystal.

Based upon this understanding of the sources of background intensity, two accurate interpolative methods for obtaining approximate background intensities were devised. Both methods allowed for significant savings of crystal X-ray exposure time, and were capable of producing background estimates of the same quality as measured background. The conclusions that air scatter was a major contributor to the background led to proposed ways of reducing or eliminating the air-scattered component (Krieger *et al.*, 1974).

Since any reduction of the background intensity is reflected directly in the peak*-to-background ratio of the measurements of diffraction maxima, the gain in reducing background scatter is significant, particularly for small crystals. If, for example, the background is reduced tenfold, then equivalent intensity data may be collected from ten times smaller crystals, although the measuring time is ten times longer. This is important when crystal size is limiting.

The first of two experimental techniques for reducing background is a simple precaution which should be taken to reduce the 'visible volume' of air which may scatter X-rays into the detector. In the second method, air in the visible volume is replaced by helium contained in a small Mylar-walled cylinder around the crystal. This device may also be conveniently used to control the temperature of the crystal.

## Experimental

Measurements were made on a Syntex $P\bar{1}$ diffractometer using copper $K\alpha$ radiation selected by reflection from a graphite monochromator. The location of restricting apertures and the running conditions of the diffractometer are summarized in Table 1.

A controlled-environment chamber was assembled and mounted on top of the goniometer head. The chamber was constructed in two parts, which are illustrated in Fig. 1. The first component, the base plate

* Contribution No. 5226. Supported by U.S. Public Health Service Grant GM-19984.

† Danforth Foundation Fellow.

‡ National Institutes of Health Career Development Awardee, U.S. Public Health Service Grant No. GM-70469.

* 'Peak' is defined to be the intensity of a diffraction maximum after correction for background.

Table 1. *Characteristic data for the diffractometer used in this study*

| Model | Syntex $P\bar{1}$ |
|---|---|
| Source | |
| Target size (mm) | 10 × 1 |
| Voltage (kV) | 40 |
| Current (mA) | 20 |
| Radiation | Cu $K\alpha$ |
| Geometry | |
| Take-off-angle | 6° |
| Monochromator type | Graphite |
| Monochromator mounting ($\varrho$)* | 90° |
| Monochromator dispersion | 0·3° |
| Source to crystal | |
| Distance from source to: | |
| 1st aperture (cm) (size in mm) | 5·5 (2·0) |
| Monochromator crystal | 6·8 |
| Aperture (size) | 19·8 (1·0–1·5) |
| Aperture (size) | 21·3 (1·5–2·0) |
| Crystal | 27·3 |
| Crystal to counter | |
| Distances from crystal to: | |
| Aperture 1 (size) | 9·0 (0–4) |
| Aperture 2 (size)† | 35·0–40·0 (5) |
| Counter | 40·5 |
| Counter | Tl-drifted NaI |
| Noise count rate with X-rays off (per 100s) | 35 |

* $\varrho$ is the angle between the normals to the planes of incidence at the monochromator.

† Aperture 2 is a 5 mm diameter tube which is 5 cm long.

*A* (illustrated in section in Fig. 1), is rigidly mounted on top of a eucentric goniometer head. A crystal can be mounted in the usual manner, with the mounting pin locked rigidly into the center of the base plate. The second part, *B*, which fits on top of the base plate, carries a cylindrical Mylar window and provides an environmental seal. Gas flow through the chamber is achieved through ports, *P*, mounted into the base plate. The temperature inside the chamber is measured using a thermistor, *T*, mounted into the top of the device, opposite the $\varphi$ drive shaft. In order to prevent condensation onto the outside of the Mylar windows, a laminar flow of dried air can be maintained on the outside of the Mylar window by leakage of air through holes in the copper tube, *C*. The laminar flow is in the direction away from the goniometer head. With this device, the environment around the crystal may be carefully controlled and monitored. Leakage from the cell is low so that a closed circuit of cooled helium gas may be recycled through the cell. A slightly greater-than-air pressure is maintained in the helium system to ensure that helium is not displaced by air.

Background intensity measurements were made both with and without the Mylar chamber; with and without a capillary, or a capillary and crystal; and with air or helium in the chamber. The effects of varying the size of counter aperture 1, located 9·0 cm from the crystal and 31·5 cm from the counter, were assessed.

Crystals of diisopropyl phosphoryl trypsin (DIPT) with dimensions 0·5 × 0·15 × 0·1 mm mounted in a 0·7 mm diameter capillary, or 0·15 × 0·15 × 0·5 mm mounted in a 0·2 mm capillary, were used in the crys-

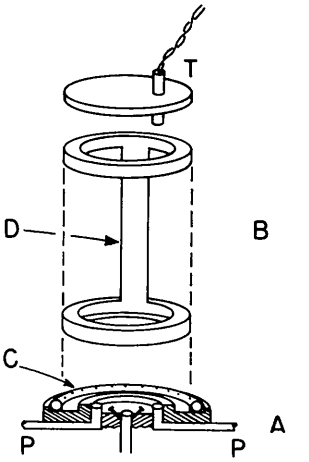


Fig. 1. Gas-flow chamber for the control of crystal environment. The base plate *A* viewed in section is attached to a goniometer head *via* a central pin and contains a coaxial mounting slot for the crystal mounting pin normally attached to a capillary tube. Gas flows through the cell *via* ports, *P*. A laminar flow of dried air can be maintained around the cell by leakage from the tube, *C*. The body of the cell, *B*, is constructed from aluminum tubing. The outer wall is 0·001 in thick Mylar. A thermistor, *T*, is mounted in the top of the cell for temperature measurement. The chamber dimensions determine the maximum $2\theta$ angle at which data can be collected. For this device data can be collected to $2\theta_{max} = 45°$. The aluminum connection between top and bottom of the cell, *D*, is adjusted so that it lies on the opposite side of the $\varphi$ drive shaft to the quadrants of the reciprocal lattice to be measured.

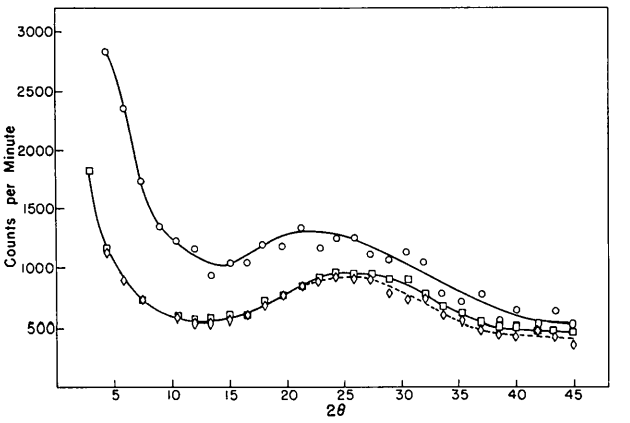


Fig. 3. The effects of changing the width of counter aperture 1 (see Table 1) on the $2\theta$ dependence of background intensity. Backgrounds were observed with air in the Mylar chamber and with a DIPT crystal in a 0·7 mm capillary. The data were measured using a wide setting of counter aperture 1 (4 mm, 15 s per point, ○), and using a smaller aperture 1 size (~2·5 mm, 5 min per point, □). Background intensity was also measured with the same capillary, but without the crystal in the beam (~2·5 mm aperture, 50 s per point, ◇). The vertical axis is corrected to counts per min.

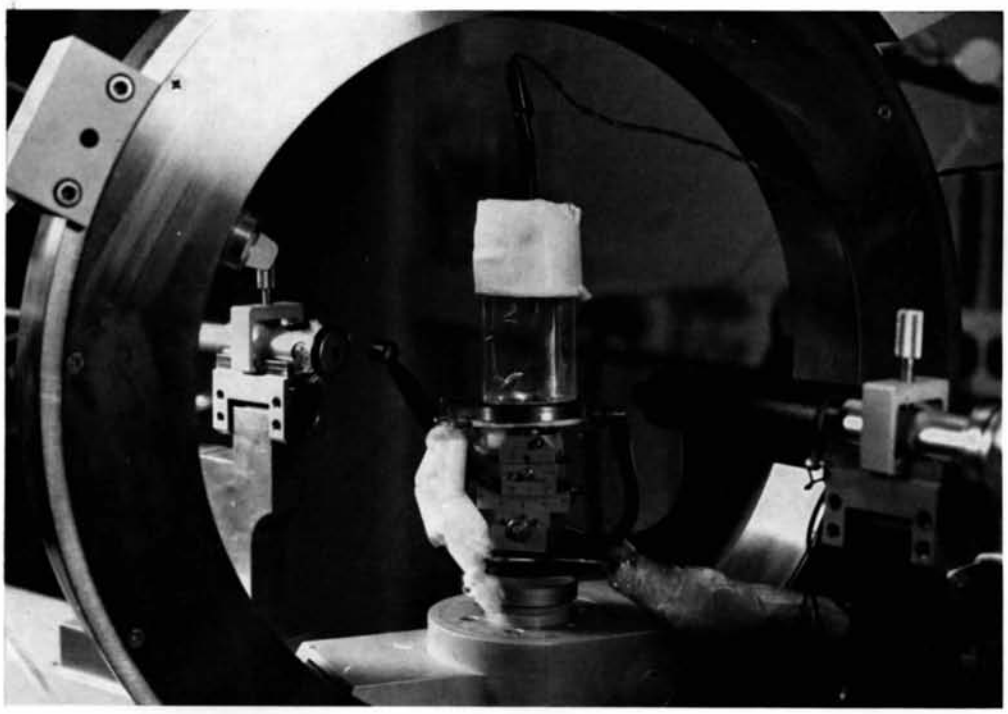

Fig. 2. The gas-flow chamber is shown mounted on the diffractometer. The variable aperture 1 is seen on the left, mounted on the detector arm.

[*To face p.* 654

tal–capillary experiments. Background counting times varied from 15 s to 10 min per point. Reflection intensities were measured in the $\omega$-scan mode. All data were collected at $\chi = 0{\cdot}0°$ and over the $2\theta$ range 2·53°–44·93°.

## Results

The diffractometer is normally equipped with only one aperture located on the detector arm immediately in front of the detector. A second (variable-sized) aperture system was fixed 9·0 cm from the crystal on the detector arm, and can be seen in Fig. 2. This aperture limits the visible volume of air in the direct beam which can radiate into the detector.

The effect of including this aperture is illustrated in Fig. 3. The upper curve represents the background intensities measured as a function of $2\theta$ for a trypsin crystal mounted in a capillary tube in the normal way. Aperture 1 is present, but is at its maximum opening of 4·0 mm across. The lower curve shows the effect of closing down the aperture to about 2·5 mm across. This represents an approximately 60% reduction in the visible volume. As a result, the background intensity at both high and low $2\theta$ angles is diminished as predicted (although the effect is clearly greatest at low angles). The dotted line shows the effect of removing the crystal from the capillary, and confirms our previous observation that background intensity is essentially independent of the crystal under normal circumstances. If there were no aperture 1, the background intensity would be even higher than that represented by the upper curve.Therefore, the addition of a second aperture on the counter arm as close as possible to the crystal significantly improves the data. This would not be true if most of the background intensity was generated by capillary and crystal. The width of aperture 1 must be large enough not to interfere with the diffracted beam.

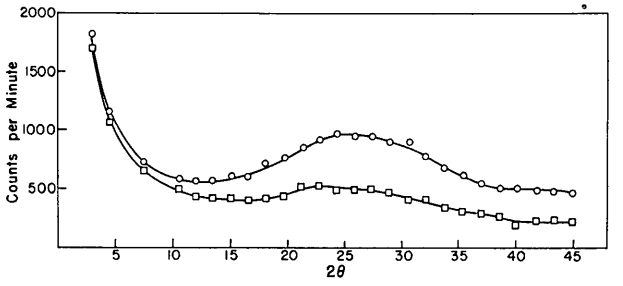


Fig. 4. The effects of capillary size on the $2\theta$ dependence of the backgrounds. Backgrounds were observed with air in the Mylar chamber, and with DIPT crystals mounted in a large (0·7 mm diameter, 5 min per point, ○), or a small (0·2 mm diameter, 1 min per point, □) glass capillary. The counter aperture width was ~2·5 mm.

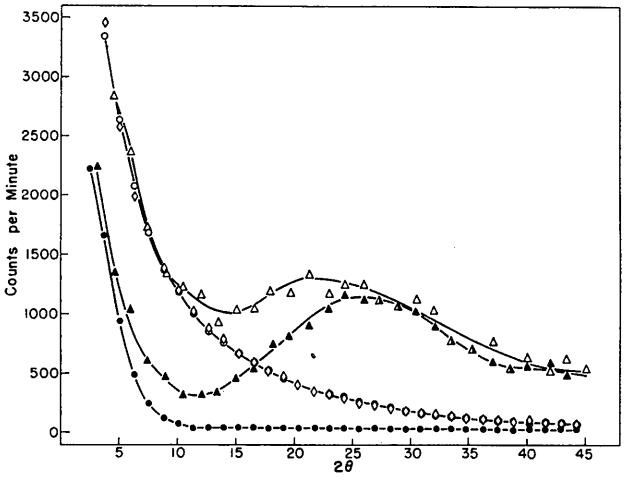


Fig. 5. The $2\theta$ dependence of backgrounds with air or helium in the Mylar chamber. (*a*) Backgrounds observed without a capillary or crystal in the beam. All points were measured for 8·33 min each either with air (○) or helium (●) in the chamber, or without the chamber (◇). (*b*) Backgrounds observed with a DIPT crystal in a 0·7 mm diameter capillary in the beam. All points were measured for 15 s each, either with air (△) or helium (▲) in the chamber. The counter aperture 1 width was 4·0 mm.

In order to effectively reduce the high-angle background due primarily to scatter from glass, the amount of glass in the direct beam must be reduced. The differences in the background between crystals mounted in 0·7 mm and 0·2 mm diameter capillaries are shown in Fig. 4. As expected, the backgrounds are similar at low $2\theta$ angles, and the smaller capillary scatters less at higher angles.

In the second series of studies, the effect of substituting helium for air in the visible volume around the capillary was assessed using the environmental chamber. Fig. 5 shows the effect of replacing the air in the visible volume with helium. In the absence of a capillary or crystal, there is an approximately 26-fold reduction in the background at $2\theta = 12°$ which diminishes to a 13-fold reduction at $2\theta = 17{\cdot}7°$ (corresponding to interplanar spacings of 5 Å). As far out as 37° in $2\theta$, the air-only background is still three times greater than the background with the helium-filled chamber. The backgrounds measured without the chamber show that the Mylar wall is essentially X-ray transparent. With a crystal and capillary in the beam, the effect of the helium-filled volume is still substantial, although capillary scattering dominates the background at high $2\theta$ angles as expected. The helium had no effect on the magnitude of the integrated reflection intensities after correction for the background.

The overall effect of adding the helium chamber, using a small capillary and minimizing the width of aperture 1, is depicted in Fig. 6. In concert, these precautions reduce the background (and therefore increase the peak-to-background ratio) by a factor of between three and ten throughout the $2\theta$ range, $2\theta = 0°$ to $2\theta = 45°$.

## Discussion

The atomic absorption coefficients of nitrogen and oxygen for Cu $K\alpha$ radiation are 17·5 and 30·5, re-

spectively (*International Tables for X-ray Crystallography*, 1968). The absorption coefficient for helium is 0·255; thus, helium absorbs less, so scatters less radiation. For helium to effectively reduce backgrounds, it must replace the air that is contributing significantly to the background. The common practice of reducing air absorption of incident or diffracted beam intensity by using helium-filled tubes which enclose the beams only slightly affects the peak-to-background ratio since the source of background intensity is not affected in any way. The main value of a helium pathway placed between the crystal and the detector is that it reduces air absorption of the diffracted beam. A 25 cm helium pathway typically increases peak intensities by about 20%. Data collection time can be reduced in direct proportion to the increase in diffracted intensity without sacrificing accuracy. By using a gas-flow chamber around the crystal, helium replaces air in the visible volume and thus directly reduces the background. For the case illustrated in Fig. 5, the air-scattered component of the background was reduced 26-fold at $2\theta = 12°$. The use of smaller capillaries or of restricting apertures close to the crystal also reduces the background because these precautions directly affect the content or the size of the visible volume. In concert, these techniques can produce a three- to tenfold reduction in the background intensity over the entire $2\theta$ range normally used for protein crystallography (out to a resolution of 2·0 Å).

When backgrounds are reduced by three to ten times, the peak-to-background ratio increases by the same factor. While changes of this magnitude have essentially no impact on the accuracy or data acquisition times for intense reflections, they can affect the collection of weak diffraction data.

The principal advantage of using background reduction techniques is that the minimum peak intensity required for statistically significant measurements is lowered as the background intensity is diminished. If the background is reduced by a factor of $f$, a small crystal can provide data equivalent to that from a crystal $f$ times larger, although the data collection time would be $f$ times longer. Alternatively, a decrease in the background will permit a reduction in the data collection time for weak reflections without loss of accuracy. Background reduction methods may also be useful in extending the resolutions of structures when the diffraction intensities rapidly become small compared to the background; for example, tRNA crystals (Kim *et al.*, 1972).

In addition to its role as a helium chamber for reducing backgrounds, the Mylar gas-flow cell provides an economical method of cooling crystals during data collection. The gas flowing through the cell can be cooled by passage through copper heat-exchange coils immersed in a cooling bath. Several other ways of cooling crystals have been described (Coppens *et al.*, 1974; Marsh & Petsko, 1973; Cucra, Singman, Lovell & Low, 1970; Streib & Lipscomb, 1962; Woodley, Hine & Richards, 1971). One difference between the gas-flow cell and cooling methods which rely on an open gas flow over the capillary and crystal is that there is essentially no condensation of atmospheric water on the moving parts of the diffractometer when the flow cell is used because the cooled gas does not flow over the instrument.

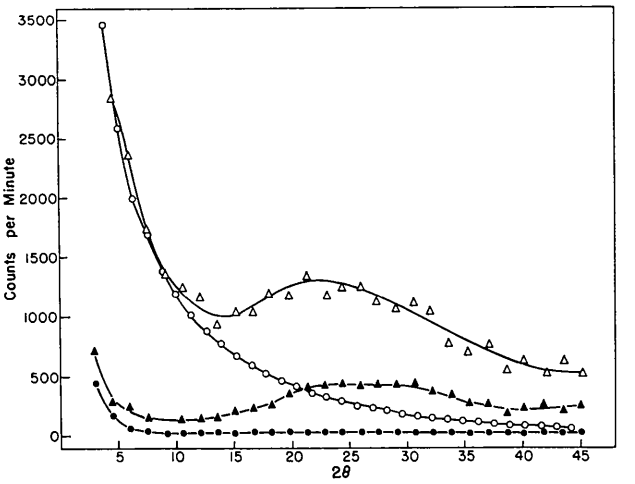


Fig. 6. The cumulative effects of the background reduction procedures on the $2\theta$ dependence of the background. (*a*) Backgrounds observed without a crystal or capillary in the beam were measured for 8·33 min per point with a 4·0 mm aperture and air in the gas-flow chamber (○) or for 5 min per point with a ~2·5 mm aperture and helium in the chamber (●). (*b*) Backgrounds observed with a DIPT-crystal in the beam were measured with the crystal mounted in a large capillary (0·7 mm diameter) with a large aperture (4·0 mm) and air in the chamber (△ – 15 s per point) or in a small capillary (0·2 mm diameter) with a smaller aperture ~(2·5 mm) and helium in the chamber (▲ – 5 min per point).

We wish to thank Mr Steven Spencer for help in the design and assembly of the gas-flow cell.

## References

Coppens, P., Ross, F. K., Blessing, R. H., Cooper, W. F., Larsen, F. K., Leipoldt, J. G. & Rees, B. (1974). *J. Appl. Cryst.* **7**, 315–319.

Cucra, P., Singman, L., Lovell, F. M. & Low, B. W. (1970). *Acta Cryst.* B**26**, 1756–1760.

*International Tables for X-ray Crystallography* (1968). Vol. III, p. 166. Birmingham: Kynoch Press.

Kim, S. H., Quigley, G., Suddath, F. L., McPherson, A., Sneden, D., Kim, J. J., Weinzierl, J., Blattmann, P. & Rich, A. (1972). *Proc. Natl. Acad. Sci. U.S.* **69**, 3746–3750.

Krieger, M., Chambers, J. L., Christoph, G. G., Stroud, R. M. & Trus, B. L. (1974). *Acta Cryst.* A**30**, 740–748.

Marsh, D. J. & Petsko, G. A. (1973). *J. Appl. Cryst.* **6**, 76–80.

Streib, W. E. & Lipscomb, W. N. (1962). *Proc. Natl. Acad. Sci. U.S.* **48**, 911–916.

Woodley, M. J. A., Hine, R. & Richards, J. P. G. (1971). *J. Appl. Cryst.* **4**, 9–12.